

Notes

# Single-Molecular Imaging of Anticoagulation Factor I from Snake Venom by Atomic Force Microscopy

XU, Xiao-Long<sup>a,b</sup>(徐小龙)      ZHOU, Yun-Shen<sup>a</sup>(周云申)      LIU, Qing-Liang<sup>\*·b</sup>(刘清亮)  
HOU, Jian-Guo<sup>a</sup>(侯建国)      YANG, Jing-Long<sup>a</sup>(杨金龙)      XIE, Yong-Shu<sup>b</sup>(解永树)

<sup>a</sup> Structure Research Laboratory, Center for Physical Sciences, University of Science and Technology of China, Chinese Academy of Sciences, Hefei, Anhui 230026, China

<sup>b</sup> Department of Chemistry, University of Science and Technology of China, Hefei, Anhui 230026, China

Anticoagulation factor I (ACF I) from the venom of *Aghistrodon acutus* is a binding protein to activated coagulation factor X (FXa) and possesses marked anticoagulant activity. Single ACF I molecule has been successfully imaged in air by tapping mode atomic force microscopy (AFM) with high-resolution using glutaraldehyde as a coupling agent. The physical adsorption and covalent binding of ACF I onto the mica show very different surface topographies. The former exhibits the characteristic strand-like structure with much less reproducibility, the latter displays a elliptic granular structure with better reproducibility, which suggests that the stability of ACF I molecules on the mica is enhanced by covalent bonding in the presence of glutaraldehyde. A small-scale AFM amplitude-mode image clearly shows that the covalently bonded ACF I molecule by glutaraldehyde has olive shape structure with an average size of 7.4 nm × 3.6 nm × 3.1 nm, which is very similar to the size determined from the crystal structure of ACF I.

**Keywords** anticoagulation factor I, atomic force microscopy (AFM), single molecule imaging, physical adsorption, covalent bonding

Anticoagulation factor I (ACF I) is a non-enzymatic anticoagulant from the venom of *Aghistrodon acutus* which has marked anticoagulant activity with a unique anticoagulant mechanism, for it forms a 1:1 complex with activated coagulation factor X (FXa) in a Ca<sup>2+</sup>-dependent fashion, and thereby blocks the amplification of the coagulation cascade.<sup>1,2</sup> ACF I is a member of coagulation factor IX/

coagulation factor X-binding protein family. In this family, the crystal structures of coagulation factor IX/factor X-binding protein (habu IX/X-bp),<sup>3</sup> coagulation factor IX-binding protein (habu IX-bp)<sup>4</sup> and ACF I<sup>5</sup> have been reported. The backbone structures of habu IX/X-bp, habu IX-bp and ACF I are almost identical with the same size of 7 nm × 3 nm × 3 nm. The ribbon model of ACF I<sup>5</sup> is shown in Fig. 1. ACF I is devoid of hemorrhagic and lethal activities, which may be useful as an effective anticoagulant, and as a convenient tool in exploration of the complex mechanisms of blood coagulation. Further study on ACF I will be valuable for designing anticoagulant drugs. In the present study, we report the topograph of the single ACF I molecule imaged by atomic force microscope (AFM).

The inventions of scanning probe microscopes (SPM) have brought about great changes for science. By means of SPM scientists have realized their hopes to directly observe single molecule.<sup>6,7</sup> Among the family of SPM, AFM has become the most popular and suitable one particularly in life science since its invention in 1986.<sup>8-13</sup> The recently invented tapping-mode and amplitude-mode atomic force microscopy made it possible to faithfully contour native proteins at a high resolution. The former has a higher vertical resolution,<sup>14</sup> while the latter has a higher lateral resolution.<sup>15</sup> In the present study, in order to directly observe the topograph of ACF I, AFM was used to

\* E-mail: qliu@ustc.edu.cn

Received November 6, 2001; revised May 13, 2002; accepted June 10, 2002.

Project supported by the National Natural Science Foundation of China (No. 20171041), the Major State Basic Research Development Program of China (No. G1999075305) and the Anhui Provincial Natural Science Foundation (No. 00044428).

successfully image single ACF I molecule. The primary investigations of effects of the physical adsorption and covalent binding of ACF I on its AFM image are also described in this paper. The results indicate that in the presence of covalent coupling reagent glutaraldehyde the high-resolution image of ACF I molecule can be obtained by amplitude-mode, which shows ACF I has olive shape structure with the average size of  $7.4 \text{ nm} \times 3.6 \text{ nm} \times 3.1 \text{ nm}$ .

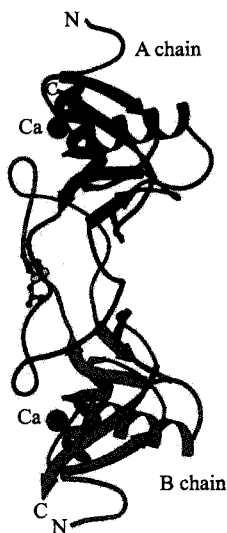


**Fig. 1** Ribbon model of the heterodimer polypeptide chains of ACF I.

## Materials and methods

### Materials

Lyophilized venom powder was provided by the TUNXI Snakebite Institute (Anhui, China). ACF I was purified by the method described previously<sup>1</sup> and shown to be homogeneous as judged by PAGE, SDS-PAGE and MALDI-TOF mass spectrometry. Purified ACF I was frozen and stored in a buffer containing Tris-HCl (pH 8.0, 20 mmol/L) and diluted to a concentration of  $1.0 \mu\text{g}/\text{mL}$  in the buffer solution (pH 8.0, 20 mmol/L Tris-HCl, 200 mmol/L NaCl) before AFM imaging. Milli-Q ultrapure water was used throughout.

### AFM imaging

A  $10 \mu\text{L}$  drop of 0.4% (V/V) glutaraldehyde solu-

tion was deposited to a freshly cleaved mica ( $\sim 5 \text{ mm} \times 5 \text{ mm}$ ) which was glued to a steel disc of 10-mm diameter and the excess solution was sucked up by filter paper. Immediately a  $10 \mu\text{L}$  of ACF I solution was punched to the mica and left to incubate for 30 s. Then the sample was gently rinsed with the corresponding buffer and subsequently, extensively with ultrapure water to remove excess molecules, and finally dried with high pure  $\text{N}_2$  gas. The sample was imaged with a commercial instrument (Nanoscope IIIa; Digital Instruments, Santa Barbara, CA) with a  $1.38\text{-}\mu\text{m}$  scanner (A-scanner) in its tapping mode or amplitude mode in air at  $20 \text{ }^\circ\text{C}$  at a relative humidity of 30%–35%. The  $160\text{-}\mu\text{m}$ -long V-shaped cantilevers purchased from Digital Instruments (Santa Barbara, CA) had a force constant of  $k = 0.032 \text{ N/m}$  and oxide  $\text{Si}_3\text{N}_4$  tips. The images were recorded at a line frequency of 2 Hz ( $512 \times 512$  pixels) and processed by flattening (using Nanoscope software) to remove background slope.

## Results

### *Imaging of ACF I physically adsorbed on to the surface of a mica*

Many biomolecules, such as proteins, can be directly adsorbed on the freshly cleaved mica from a buffer solution through the van der Waals force, the electrostatic double-layer force, as well as the hydrophobic effect. Once the molecules are adsorbed, specific interactions like hydrogen bonds or salt bridges can arise. Some proteins can be strongly adsorbed on the freshly cleaved mica by physisorption and can be imaged by AFM. In order to analyze the physisorption of ACF I to mica, a  $10 \mu\text{L}$  of  $1.0 \mu\text{g}/\text{mL}$  ACF I solution (200 mmol/L NaCl, 20 mmol/L Tris-HCl, pH 8.0) was directly deposited on a freshly cleaved mica. After washed with the corresponding buffer and then extensively with ultrapure water and finally dried with  $\text{N}_2$ , the sample was imaged with AFM in tapping mode. Fig. 2 shows the topography image in tapping mode of ACF I molecules physically adsorbed onto mica, which show strand-like features. These strand-like features varied greatly in length with an average of 46 nm. A typical character of these strand-like was their orientations which were horizontal to the scanning direction of AFM tip. The results suggest that the physisorption of ACF I to mica is not firm enough and the single ACF I

molecule is easily to be deformed or pushed away by the AFM stylus during raster scanning of the surface. Because the strong damage or deformation of the samples by sharp tip required for high resolution, it is impossible to exactly measure the size of single ACF I molecule from the image. The strand-like structures were also found to change with the loading force and the scanning speed. Both the increase of scanning speed and the decrease of loading forces resulted in slight shortening of lengths of strands, but they also gave adverse effects on the image resolution of ACF I.

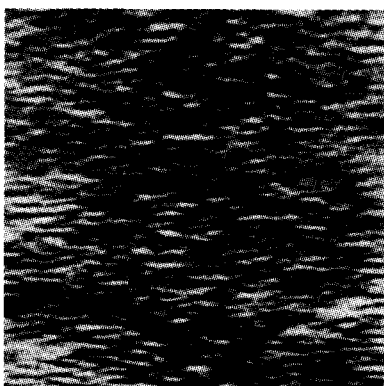


**Fig. 2** Image of ACF I physically adsorbed on mica at the concentration of 1.0  $\mu\text{g}/\text{mL}$  by tapping mode AFM at 20  $^{\circ}\text{C}$  (scan area: 1000 nm  $\times$  1000 nm, z-range: 0–10 nm).

#### *Imaging of ACF I covalently immobilized onto the surface of a mica*

In order to obtain high resolution image of ACF I, glutaraldehyde (Glu), a common coupling reagent, was used to covalently immobilize ACF I onto a mica. As shown in Fig. 3, the ACF I molecules covalently attached to the mica exhibited, in most cases, elliptic granular structures in the AFM images. These elliptic granular structures were stable with continuous scanning under the experimental conditions. Mostly, the sizes of these granules are similar, typically average 2.8 nm in vertical height and 24.8 nm  $\times$  19.0 nm in lateral dimensions. In the AFM, frequently structures of biomolecules like proteins appear broadened because of the finite size of the tips. So these tip broadening effects must be taken into account. In the experiment, the radius of curvature of the tip is 10 nm. The feature radius ( $r_{\text{feature}}$ ) can be calcu-

lated by Eq. (1).<sup>16</sup>

$$d_{\text{AFM}} = 4(r_{\text{tip}}r_{\text{feature}})^{1/2} \quad (1)$$

where  $r_{\text{tip}}$  is the tip radius of curvature and  $d_{\text{AFM}}$  the measured feature diameter. Using a value of  $r_{\text{tip}} = 10$  nm, the average feature lateral diameters were calculated to be 7.7 nm  $\times$  4.5 nm.

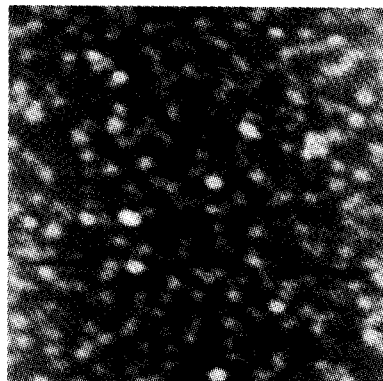


**Fig. 3** Image of ACF I covalently immobilized onto mica by 0.4% (V/V) Glu at the ACF I concentration of 1.0  $\mu\text{g}/\text{mL}$  by tapping mode AFM at 20  $^{\circ}\text{C}$  (scan area: 600 nm  $\times$  600 nm, z-range: 0–5 nm).

When proteins adsorb on a substrate, the high concentration of proteins may give rise to the aggregation of proteins which cause more ACF I molecules to loosely adsorb onto mica and give adverse effects on the image resolution of ACF I. On the other hand, the dense proteins close or connect with others on mica surface which make against imaging single molecules. In order to achieve high resolution image of ACF I, the concentration of ACF I was decreased to 0.1  $\mu\text{g}/\text{mL}$  to reduce the surface density of ACF I on mica substrate. In addition, a smaller tip with curvature radius of 5 nm was used to record the image of ACF I by amplitude-mode. Amplitude-mode image can enhance contrast at the edges of features and has a higher resolution at feature edges as opposed to the tapping mode image.<sup>15</sup> A small-scale AFM amplitude-mode image clearly shows randomly distributed ACF I molecules on the mica mostly with characteristic olive shape structures (Fig. 4), which have the average vertical height 3.1 nm and the average lateral dimensions 17.2 nm  $\times$  12.0 nm for three features indicated by the arrows in Fig. 4. The average lateral dimensions of the feature of ACF I

were calculated to be  $7.4 \text{ nm} \times 3.6 \text{ nm}$  from the measured data by Eq. (1).

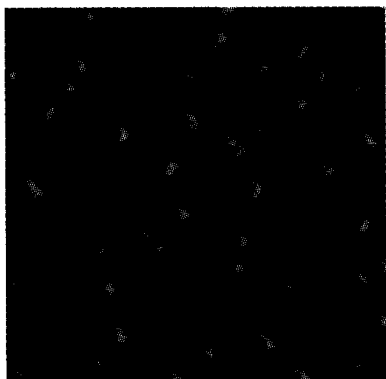


**Fig. 4** AFM image of ACF I covalently immobilized onto mica by 0.4% (V/V) Glu at the ACF I concentration of  $0.1 \mu\text{g/mL}$  by amplitude mode at  $20 \text{ }^\circ\text{C}$  (scan area:  $300 \text{ nm} \times 300 \text{ nm}$ , z-range:  $0\text{--}6 \text{ nm}$ ).

## Discussion

Protein molecules immobilized on substrates can interact with the surfaces by either physisorption (nonspecific manner) or covalent adsorption (specific manner). Some proteins can be strongly adsorbed on substrates by physisorption and can be imaged by AFM, while the weakly adsorbed protein molecules in the nonspecific manner can contaminate the scanning tip and give rise to an increase of interactions between the tip and the protein, and thereby are usually displaced or manipulated under the forces exerted by the scanning tip and affect adversely the resolution of AFM imaging of protein. ACF I adsorption to a mica in the absence of coupling reagent, is nonspecific adsorption. The weak electrostatic and/or hydrophobic forces are primarily involved in the interactions between the ACF I molecules and the mica. The strand-like features of ACF I physically adsorbed on mica indicate that the physisorption of ACF I to mica is not firm enough for its AFM image. The dependency of the strand-like structures on the scanning rates suggests that the interaction between the tip and ACF I molecules can be reduced by the increase of the scanning rate to some extent, but the high scanning rate results in the decrease of resolution of ACF I image. Although some loosely adsorbed molecules can be removed off by gentle washing the mica with the corresponding buffer solution, the buffer

solution can not remove all the weakly adsorbed molecules. As a result, the strand-like structures were observed. Therefore, ACF I can not be clearly imaged in physisorption manner.

In order to obtain high-resolution images of protein molecules using AFM, the molecules should be firmly attached to resist the destructive force exerted by the scanning tip. The covalent coupling can significantly decrease the number of loosely adsorbed protein. It was performed via effective covalent binding with Glu in our experiments. Once the molecules are bound, other interactions like hydrogen bonds, salt bridges or hydrophobic interaction forces between ACF I and mica also take place. The results show that AFM image in this case has a higher resolution and reproducibility than that in the absence of coupling reagent, which suggests the stability of ACF I molecules on the mica is enhanced by covalent bonding in the presence of Glu.

Each ACF I molecule takes somewhat different shapes due to its inherent flexibility and different orientations to the mica. Although ACF I used in the experiment was detected to be high pure, the images of each molecule are not identical even in the presence of Glu. The lateral and vertical dimensions of ACF I vary from molecule to molecule. In most cases, the image of ACF I in the presence of Glu shows an olive shape structure with  $3.1 \text{ nm}$  in average vertical height and  $7.4 \text{ nm} \times 3.6 \text{ nm}$  in average lateral dimensions after deduction of the effect of tip broadening, within experimental errors, which is very similar to the size of  $7 \text{ nm} \times 3 \text{ nm} \times 3 \text{ nm}$  determined from the crystal structure of ACF I.<sup>5</sup> This result clearly shows that the topograph of single ACF I molecule can be imaged effectively and directly by AFM. Because ACF I molecule takes the shape of olive, it can be connected with the mica in the larger area and therefore can more strongly adsorb on the mica. In contrast when it stands erectly on the mica it can be connected with the mica in the smaller area and therefore more weakly adsorbs on the mica. Obviously, in order to strongly adsorb on the mica, ACF I molecule should lie on the mica. As a result, most ACF I molecules show olive-shape structures in the AFM image.

## Conclusion

We have succeeded in observing single ACF I molecule in air by tapping mode AFM with high-resolution

using Glu as a coupling agent. The physical adsorption and covalent binding of ACF I onto the mica show very different surface topographies. The former exhibits the characteristic strand-like structure with much less reproducibility, the latter displays a elliptic or olive granular structure with better reproducibility and a typical size of  $7.4 \text{ nm} \times 3.6 \text{ nm} \times 3.1 \text{ nm}$ , which is very similar to the size determined from the crystal structure of ACF I.

## References

- 1 Xu, X. L.; Liu, Q. L.; Xie, Y. S.; Wu, S. D. *Toxicol.* **2000**, *38*, 1517.
- 2 Xu, X. L.; Liu, Q. L.; Xie, Y. S. *J. Protein Chem.* **2001**, *20*, 33.
- 3 Mizuno, H.; Fujimoto, Z.; Koizumi, M.; Kano, H.; Ato-da, H.; Morita, T. *Nat. Struct. Biol.* **1997**, *4*, 438.
- 4 Mizuno, H.; Fujimoto, Z.; Koizumi, M.; Kano, H.; Ato-da, H.; Morita, T. *J. Mol. Biol.* **1999**, *289*, 103.
- 5 Liu, S.-J. *Ph. D. Thesis*, University of Science and Technology of China, Hefei, **2000** (in Chinese).
- 6 Hou, J. G.; Li, B.; Yang, J. L.; Zhu, Q. S. *Chin. Sci. Bull.* **2000**, *45*, 1912 (in Chinese).
- 7 Hou, J. G.; Yang, J. L.; Wang, H. Q.; Li, Q. X.; Zeng, C. G.; Yuan, L. F.; Wang, B.; Chen, D. M.; Zhu, Q. S. *Nature* **2001**, *409*, 304.
- 8 Binnig, G.; Quate, C. F.; Gerber, C. *Phys. Rev. Lett.* **1986**, *56*, 930.
- 9 Feng, X. Z.; Lin, Z.; Wang, C.; Bai, C. L. *Sci. China, Ser. C*, **1999**, *42*, 136.
- 10 Zhang, Y.; Chen, S. F.; Ouyang, Z. Q.; Hu, J.; Xiong, Q. H.; Li, B.; Huang, Y. B.; Li, M. Q.; Jin, C. Z. *Chin. Sci. Bull.* **2000**, *45*, 1365.
- 11 Misevic, G. N. *Methods Mol. Biol.* **2000**, *139*, 111.
- 12 Osmulski, P. A.; Gaczynska, M. *J. Biol. Chem.* **2000**, *275*, 13171.
- 13 Engel, A.; Lyubchenko, Y.; Müller, D. J. *Trends Cell Biol.* **1999**, *9*, 77.
- 14 Möller, C.; Allen, M.; Elings, V.; Engel, A.; Müller, D. J. *Biophys. J.* **1999**, *77*, 1150.
- 15 Parbhu, A. N.; Bryson, W. G.; Lal, R. *Biochemistry* **1999**, *38*, 11755.
- 16 Dong, Y. Z.; Shannon, C. *Anal. Chem.* **2000**, *72*, 2371.

(E011066 SONG, J. P.; LING, J.)